

Synthesis and application of a surface ionic imprinting polymer on silica-coated Mn-doped ZnS quantum dots as a chemosensor for the selective quantification of inorganic arsenic in fish

Kamal K Jinadasa, Elena Peña-Vázquez, Pilar Bermejo-Barrera, Antonio Moreda-Piñeiro*

Trace Element, Spectroscopy and Speciation Group (GETEE), Strategic Grouping in Materials (AEMAT), Department of Analytical Chemistry, Nutrition and Bromatology, Faculty of Chemistry, Universidade de Santiago de Compostela. Avenida das Ciencias, s/n. 15782, Santiago de Compostela, Spain

Abstract

A novel room temperature phosphorescence chemosensor probe has been successfully developed and applied to the selective detection and quantification of inorganic arsenic (As(III) plus As(V)) in fish samples. The prepared material (IIP@ZnS:Mn QDs) was based on Mn-doped ZnS quantum dots coated with (3-aminopropyl) triethoxysilane and an As(III) ionic imprinted polymer. The novel use of vinyl imidazole as a complexing reagent when synthesizing the ionic imprinted polymer guarantees that both inorganic arsenic species (As(III) and As(V)) can interact with the recognition cavities in the ionic imprinted polymer. After characterization, several studies were performed to enhance the interaction between the targets (As(III) and As(V) ions) and the IIP@ZnS:Mn QDs nanoparticles. The optimization and validation process showed that the composite material offers high selectivity (high imprinting factor) for inorganic arsenic species. The limit of quantification for total inorganic As was $29.6 \mu\text{g kg}^{-1}$, value lower than the EU/EC regulation limits proposed for other foodstuffs than fish, such as rice. The proposed method is therefore simple, requires short analysis times and offers good sensitivity, precision (inter-day relative standard deviations lower than 10%), and quantitative analytical recoveries.

* Corresponding author E-mail: antonio.moreda@usc.es; phone: +34881814375; ORCID: orcid.org/0000-0002-3512-6434

The method has been successfully applied to assess total inorganic arsenic in several fishery products, showing good agreement with the total inorganic arsenic concentration (As(III) plus As(V)) found after applying other advanced and expensive methods such those based on high performance liquid chromatography hyphenated to inductively coupled plasma – mass spectrometry.

Keywords

Silica-coated Mn-doped ZnS quantum dots, ionic imprinted polymer, room temperature phosphorescence, inorganic arsenic, fish, chemosensor probe

1. Introduction

Arsenic (As) is one of the major global environmental pollutants and it is a naturally occurring element at trace levels in the air, water, soil, and in animals and plants [1]. The Agency for Toxic Substances and Disease Registry (ATSDR) of the United States ranked arsenic as number one in their Substance Priority List in 2017, while the International Agency for Research on Cancer (IARC) has classified arsenic as a class one carcinogen due to the existence of sufficient evidence of human carcinogenic effect [2,3]. Food and water are the main pathways for As exposure in human population. Moreover, seafood and fish are one of the major contributors to As in the diet [4]. The toxicity and bioavailability of As depends on its concentration and chemical form; hence, speciation data is essential to define the toxicological endpoint [5]. Arsenobetaine (AsB) is considered a non-toxic form and it has been identified to be the major arsenical in seafood, while other organic toxic As species such as monomethyl arsenic (MMA), dimethyl arsenic (DMA), and most toxic inorganic As species such as arsenite [As(III)] and arsenate [As(V)] have been also found in seafood and fish [6].

Semiconductor nanocrystals or quantum dots (QDs) have been widely used as probes for recognizing and sensing molecules [7,8] because of their unique optical and electronic properties such as large surface-to-volume ratios, high luminescence efficiency, narrow symmetric emission and excellent photostability and quantum-size effects [9,10]. Inherent luminescent properties of QDs make them to be appealing materials for chemosensors development as reviewed by Costa-Mora et al. [11]. Most of applications, however, have exploited the QDs' fluorescent properties, and little attention has been paid to room temperature phosphorescence (RTP). The main advantage of RTP is the longer luminescence (RTP) lifetime, which helps to avoid interferences from auto-fluorescence and scattering light, and increases detection reliability [8]. Therefore, some doped (functionalized) semiconductor systems based on RTP have been developed for the detection of several molecules and metal ions such as acetone in water and urine [12], thiram residues in fresh fruit peels [13], and 2,4,6-trinitrotoluene [8], sulfide [14], Hg(II) [15], Pb(II) [16], and Mn(VII) [17] in water samples.

However, selectivity of QDs-based chemosensors has been reported to be poor and the methods are not straightforward for complex samples. Selectivity improvement can be easily reached when combining Molecular Imprinting Technology (MIT) with QDs. MIT is an appealing technique to design tailor-made materials with high selectivity for a target molecule (Molecularly Imprinted Polymers, MIPs) [18], or for a target ion (Ionic Imprinted Polymers, IIPs) [19]. The synthesis of MIP/IIP-QD composites becomes therefore a hot spot in analytical science because allows overcoming the problems related to the lack of selectivity of QD measurements, and offers sensitive determinations based on the inherent QDs' luminescent properties. Recent reviews on this issue show an increasing number of MIP-QDs-based fluorescence methods for the selective detection of organic compounds [20,21].

Despite IIPs have been used for selective adsorbents in solid phase extraction (SPE) procedures [19], there are few developments for IIP-QD composites for metal ions sensing. To the best of our knowledge, there are only two recent developments combining IIP and QDs for fluorescence

sensing of Cu(II) and Hg(II) in water [22] and Cr(VI) in aqueous solutions [23]. The approach performed by Qi et al. [22] consists of grafted IIP-CdTe QDs for a fluorescence multiplexed detection of Cu(II) and Hg(II) ions; whereas, Cr(VI) detection was carried out by Mn-doped ZnS QDs [23]. Sensitive and selectivity RTP chemosensors based on IIP-QDs have still not been developed, and our studies are the first RTP probe for metal ions and also the first for inorganic arsenic (As(III) and As(V)). The use of a bifunctional monomer such as 1-vinyl imidazole allows selective recognition cavities for the template ion (As(III)) and also for As(V), structurally similar ions, which generate a selective chemosensor for inorganic As species (both inorganic As species are highly toxic species). The chemosensor system proposed is therefore less expensive than methodologies based on high performance liquid chromatography (HPLC) and atomic spectrometric techniques (mainly inductively coupled plasma – mass spectrometry, ICP-MS), and requires a simple sample pre-treatment. The development of new methods for detecting inorganic As in fish with convenience, low cost, high sensitivity, and fast analysis is a great challenge. To the best of the authors' knowledge, the current research is the first attempt to develop a phosphorescent IIP-QDs composite for the detection and quantification of total inorganic As. High sensitive and selective total inorganic As can be attained using low-cost instrumentation such as those based on phosphorescence measurements.

2. Materials and methods

2.1. Reagents

All chemicals and reagents used were of analytical grade or better, and they were used as received in the lab, except 2,2'-azobisisobutyronitrile (AIBN) and divinylbenzene (DVB), both reagents from Sigma Aldrich (Steinheim, Germany), which were subjected to a further purification procedure (polymerization inhibitor removal according to Chantada-Vázquez et al [24]). Briefly, AIBN was purified by crystallization at -20 °C after dissolving the reagent in

Chromasolv methanol (Merck, Darmstadt, Germany) at 50-60 °C. DVB reagent was passed throughout a mini column containing 0.50 g of neutral alumina (Merck). All aqueous solutions were prepared with ultrapure water with a resistivity of 18.2 M Ω cm⁻¹ (Milli Q-A10, Millipore, Bedford, MA, USA). Mn-doped ZnS QDs were synthesized using zinc sulphate heptahydrate (Panreac, Barcelona, Spain), manganese dichloride (Merck) and sodium sulfide hydrate from Fluka (Buchs, Switzerland). APTES (3-aminopropyl)-triethoxysilane, powdered sodium(meta)arsenite, and 1-vinyl imidazole were from Sigma Aldrich. Arsenite and arsenate stock standard solutions, 1000 mg L⁻¹, were from Panreac. Standard solutions of monomethyl arsenic (MMA), dimethyl arsenic (DMA), arsenobetaine (AsB) and arsenocholine (AsC) (1000 mg L⁻¹) were prepared by dissolving the appropriate amounts of MMA (Carlo Erba, Milan, Italy), DMA (Merck), and AsB and AsC (Tri Chemical Laboratory Inc, Yamanashi, Japan).

Nitric acid (Hyperpur, 69%), 33% hydrogen peroxide, acetic acid, and ethanol were supplied by Panreac; whereas, ammonium dihydrogen phosphate was from BDH (Poole, United Kingdom). NexIon Setup Solution (10 μ g L⁻¹ of Be, Ce, Fe, In, Li, Mg, Pb, and U in 1% HNO₃) was purchased by Perkin Elmer (Shelton, CT, USA). Multi-element standard solutions (cross-reactivity studies) were prepared by combining single Ca, Co and Mg stock standard solutions (1000 mg L⁻¹) from Merck, single Cr, Hg, K, P, Pb and Zn, stock standard solutions (1000 mg L⁻¹) from Scharlab (Barcelona, Spain), and single Cd, Cu, Fe and Na stock standard solutions (1000 mg L⁻¹) from Perkin Elmer. Internal standard (Ge) for ICP-MS measurements were prepared from a single-element standard (1000 mg L⁻¹) purchased from Perkin Elmer. 1-hexyl-3-methylimidazolium was purchased from IoLiTec Ionic Liquids Technologies, (Heilbronn, Germany). The BCR-668 (mussel tissue) certified reference material (CRM) was from the European Commission Joint Research Centre, Institute for Reference Materials and Measurements (Geel, Belgium).

Other consumables were Durapore 0.20 μ m membrane filters (Millipore), disposable syringes (sterile, 5 mL) (Dispomed, Gelnhausen, Germany), replacement polytetrafluorethylene frits (20

μm porosity for use with 6 mL glass SPE tubes) from Supelco (Bellefonte, USA), and cellulose acetate 0.45 μm syringe filters (Labbox Labware S.L., Barcelona, Spain).

2.2. Instrumentation

Morphology of synthesized IIP-QDs was assessed by transmission electron microscopy – energy-dispersive spectroscopy (TEM-EDS) using a JEM-2010F (JEOL, (Tokyo, Japan) equipped with an IncaEnergy TEM detector (Oxford Instruments, High Wycombe, United Kingdom) operating as high-angle annular dark-field scanning transmission electron microscopy (HAADF-STEM). Microstructure of the prepared material was assessed by X-ray diffraction spectrometry (XRD) using an EMPYREAM instrument from PaNalytical (Almelo, Netherlands). A Spectrum-Two FT-IR spectrometer from Perkin Elmer (Waltham, MA, USA) operating at the attenuated total reflectance (ATR) mode was also used for characterizing the synthesized material.

A Cary Eclipse fluorescence spectrophotometer from Varian (Victoria, Australia) equipped with a xenon discharge lamp and 10 mm quartz cells and operating in phosphorescence mode was used for RTP measurements. Single determination of inorganic As species (III and V) by HPLC-ICP-MS were performed with a Flexar high-performance liquid chromatograph hyphenated to a NexION 300 inductively coupled plasma mass spectrometer (Perkin Elmer, Waltham, USA). The As species were separated using a PRP \times 100 column (10 μm , 4.1 \times 100 mm) from Hamilton (Reno, NV, USA). The same ICP-MS instrument connected to a SeaFast SC2DX autosampler (Elemental Scientific, Omaha, NB, USA) was also used for total As determination after microwave assisted acid digestion of fish samples using a Milestone Ethos Plus high-performance lab station (Sorisolet, BG, Italy).

An ASE150 accelerated solvent extractor (Dionex Corporation, Sunnyvale, CA, USA) was used for template removal from IIP-QDs nanoparticles. An USC60TH ultrasonic cleaner bath (45 kHz, 120 W) from VWR (Leuven, Belgium), an ultracentrifuge (Sigma 2K15, Osterode, Germany), a Basic 20 pH meter with glass combined electrode (Crison, Barcelona, Spain), a

domestic Taurus blade grinder (Taurus, Barcelona, Spain), an oven model 207 from Selecta (Barcelona, Spain), and a Classic ML analytical balance (Metler Toledo, Columbus, OH, USA) were used throughout this research.

2.3. Synthesis of IIP@ZnS:Mn QDs

Water-soluble IIP coated Mn-doped ZnS QDs (IIPs@ZnS:Mn QDs =IIP-QDs) were synthesized via the procedure explained by Ren and Chen [25] with some modifications. The procedure includes four steps:

(1) Briefly, 12.5 mmol $\text{ZnSO}_4 \cdot 7\text{H}_2\text{O}$, 1 mmol of MnCl_2 and 40 mL of ultrapure water were placed into a three-neck flask under ultrasonication and N_2 stream. After 10 min, 10 mL of 1.25 mmol of Na_2S was added dropwise using an addition funnel. The ultrasonication continued for 30 min, and then 2.5 mL of APTES was added. Afterwards, ultrasonication was kept for 4.5 h under the N_2 stream. The synthesized Mn-doped ZnS QDs were isolated by centrifugation at 3000 rpm for 20 min. The centrifugation step was repeated 3 times, washing with 5 mL ethanol between each step. Synthesized nanoparticles were dried inside a desiccator in the dark, and finally stored at 4 °C.

(2) A pre-polymerization mixture was prepared by dissolving 1.5 mmol of NaAsO_2 and 6.5 mmol of vinyl imidazole in 10 mL of acetic acid in methanol (25 % v/v), sparging with N_2 . The mixture was stored in the dark for 12 h to facilitate template and monomer assembly. The template was not used in this step for the synthesis of the non-imprinted polymer (NIP).

(3) The third step of the synthesis consists of mixing approximately 0.5 g of ZnS:Mn doped QDs with the pre-polymerization mixture (10 mL of of 25%(v/v) acetic acid in methanol containing NaAsO_2 and 1-vinyl imidazole), 32 mmol of DVB, 25 mL ultrapure water, and 40 mg of AIBN. The polymerization was carried out for 5 h under ultrasounds. Finally, the IIP-QDs were cleaned with 60 mL of ethanol, dried and stored in the dark at 4 °C.

(4) Template removal is a critical procedure in the IIP-QDs synthesis process. Three different procedures were tested to remove the template (NaAsO_2) by using an aqueous solution of ionic

liquid (IL) 1-hexyl-3-methylimidazolium acetate at 1% (m/v) as an extractant. In the first procedure, 0.5 g of IIP-QDs were packed into 5 mL syringes (polymer material between polytetrafluorethylene frits), and a volume of 750 mL of the IL solution was passed at a 0.5 mL min⁻¹ flow rate. In the second procedure, a mass of 0.5 g of IIP-QDs was placed into a beaker and stirred with 50 mL of IL solution for 6 h (the process was repeated 10 times with fresh extractant solution). In the third method, a mass 0.5 g of IIP-QDs was introduced into the ASE cell and the extraction was carried out during 7 cycles (temperature 80 °C, pressure 1500 psi, extraction time 10 min, extraction volume 20 mL). Negligible NaAsO₂ amounts (As(III) concentrations by ICP-MS) were found in the final washing solution after the application of any of the procedures. The ASE procedure is a quick and easy-to-use method; however, the resulted IIP-QDs were less stable when suspended in the aqueous solution than those IIP-QDs after template removal by using the other two methods. This may be due to high pressure of the ASE. Therefore, on-column and stirring procedures were finally selected for template removal.

2.4. Phosphorescence measurements

Measurements were carried out in phosphorescence scan mode at room temperature (20-25 °C). The excitation and emission slit widths were 10 nm and 20 nm, respectively. The photomultiplier voltage was set as a medium, while excitation wavelength (289 nm) and emission wavelength (595 nm; scan started at 520 nm and ended up at 720 nm) were selected. Moreover, the acquisition parameters in phosphorescence mode (total decay time, number of flashes, delay time and gate time) were 0.006 s, 1, 0.1 ms and 3.0 ms, respectively. All the measurements were carried out with the appropriate quantity of IIP-QDs or NIP@ZnS:Mn QDs (NIP-QDs) dispersed in a constant volume of 0.1M/0.1M KH₂PO₄-NaOH solution. The determination of inorganic As (III and V) was based on the decrease on the phosphorescence intensity (quenching effect) when these ions are present and interact with the recognition cavities of the IIP layer over the luminescent QDs.

2.5 Analysis of samples

Fish samples were obtained from local markets in Santiago de Compostela, and the following species were studied: yellowfin tuna (*Thunnus albacares*), swordfish (*Xiphias gladius*), blue shark (*Prionace glauca*) and cod (*Gadus morhua*). Inorganic arsenic extraction was performed using the following procedure: Approximately, 1.0 g of homogenate fish sample (0.2 g of CRM) was mixed with 5 mL of ultra-pure water under ultrasounds for 30 min. The mixture was then centrifuged (3000 rpm, 10 min), and the supernatant was decanted. The above procedure was repeated twice, and supernatants were combined and filtered before RTP and HPLC-ICP-MS (method used for comparison purposes, details in Table S1, electronic supplementary information ESI) measurements.

For total As assessment in fish, samples were acid digested by using microwave assistance. Briefly, 1.0 g of fish sample (0.2 g of CRM) was placed in the microwave reactors and pre-digested with 3.0 mL of 69 % (v/v) HNO₃, 4.0 mL of ultrapure water and 1.0 mL of H₂O₂ for 15 min at room temperature. Pre-digested samples were then subjected to microwave by increasing the temperature from room temperature to 180 °C for 15 min, followed by a treatment at this temperature for 10 min. Acid digests were then made up to 25 mL with ultrapure water, and they were stored in polyethylene bottles at room temperature before ICP-MS analysis (operating conditions in Table S2, ESI).

3. Results and Discussion

3.1. Preparation and characterization of IIP/NIP@ZnS:Mn QDs

Silica coating core-shell rational design has been developed for synthesis nanomaterials with versatile advantages [8]. Silica is considered as ‘generally recognized as a safe’ (GRAS) by the United States Food and Drug Administrator (US-FDA) due to low toxicity [26]. APTES (3-aminopropyl) triethoxysilane) and TEOS (tetraethoxysilane) are the most common used silica-based compounds and they are applied to enhance the mechanical stability of colloidal particles

[27]. These reagents also offer good biocompatibility, non-swelling properties, and low cost [27]. Moreover, silica-coated nanomaterials improve wettability, and also surfaces can easily be modified with bio-conjugators [28]. Additionally, silica is facilitated to increase in size by 'seed-growth' process, chemically inert, and optically transparent [29], and APTES could also act as functional monomer for further IIP and MIP synthesis.

The synthesis of IIP-QDs and NIP-QDs (Figure 1) requires the use of APTES coated ZnS:Mn QDs synthesis before the formation of ionic imprinted polymer films onto the surface of QDs using NaAsO₂ as a template ion and 1-vinyl imidazole as a bifunctional monomer. The use of bifunctional vinylated compounds guarantees the presence of vinyl groups for further polymerization, and also the presence of functional groups for interaction (complexation) with the ion (template). In the case of 1-vinyl imidazole, the presence of two nitrogen atoms in the structure allows the interaction with As(III) ions and also with As(V) ions, as will be demonstrated when studying the imprinting and selectivity factors (section 3.3.). As reported by Tsoi et al [32], 1-vinyl imidazole based As-IIPs have superior selectivity and analyte recognition than those IIPs obtained when using other monomers such as styrene and vinylated pyridine.

FTIR spectra (400-4000 cm⁻¹) of IIP-QDs (before and after removing template) and NIP-QDs are shown in Figure 2. The bands from 1000-1150 cm⁻¹, 790-795 cm⁻¹, and 470 cm⁻¹ are attributed to the asymmetric and symmetric stretching vibration of Si-O-Si, and Si-O of SiO₂. The peaks at 2923 cm⁻¹ and 2853 cm⁻¹ are due to C-H stretching vibration of the propyl group [30,31]. In addition, the characteristic peak at 610 cm⁻¹ is assigned to the ZnS band [24]. Moreover, the weak absorption peaks at 1638 and 1456 cm⁻¹ are assigned to the C=C and C≡N structure of the aromatic imidazole ring [32]. These findings prove that IIP and NIP layer was efficiently anchored onto the surface of the APTES-ZnS:Mn QDs.

XRD was used to study the purity and crystalline structure of the nanoparticles. Figure S1 (ESI section) showed the X-ray diffraction pattern of the IIP-QDs (before and after template removal), and NIP-QDs. The XRD pattern of ZnS QD showed broad diffraction β-ZnS peaks at 2θ values

of 28.74°, 47.7° and 56.5° which correspond to the cubic structure with peaks assigned to 111, 220 and 311. These figures agree with those reported by Mohagheghpour et al. [33] regarding Zn_{1-x}Mn_xS QDs. The mean crystallite size after using the Debye–Scherrer equation [34] was estimated to be 17.2±1.5 Å (1.7±0.02 nm) for IIP-QD before template removal and 19.3±2.3 Å (1.9±0.02 nm) for IIP-QD after template removal. These findings show that the template removal process did not affect the crystalline structure.

The structure of the QDs was examined by TEM, and IIP/NIP-QDs particles were found to be agglomerated spheres covered with the polymer (NIP and IIP) as shown in Figure 3A-C. EDS analysis (Figure S2A-C, ESI section) confirms the presence of Zn, S, Mn, and Si in the prepared composites, and also the presence of As in IIP-QDs before template (As(III)) removal (Figure S2B, ESI section).

3.2. Variables affecting the RTP quenching by inorganic arsenic species

3.2.1 Effect of the interaction time between inorganic As and IIP-QDs

In order to investigate the influence of the interaction time between As(III) ions and IIP-QDs on RTP intensity, an aqueous IIP-QDs (50 mg L⁻¹) solution was prepared in 0.1 M KH₂PO₄/0.1 M NaOH (pH 8.0), and then 1.5 mL aliquots of the prepared IIP-QDs solution were mixed with 40 µL of aqueous As (III) at 500 µg L⁻¹ prepared in 0.1 M KH₂PO₄/0.1 M NaOH (pH 8.0) and 460 µL prepared in 0.1 M KH₂PO₄/0.1 M NaOH (pH 8.0) which yields to an As(III) concentration of 10 µg L⁻¹ after dilution in the screw-capped vials (40 µL to 2.0 mL). The RTP intensity was measured until 30 min in 2 min intervals and RTP intensity was found to be stable after 15 min. Therefore, 15 min was selected as interaction time for further experiments.

3.2.2. Effect of the pH

The effect of the pH on RTP intensity was studied within the 5.0-8.0 pH range by preparing IIP-QDs (50 mg L⁻¹) solutions in 0.1 M KH₂PO₄/0.1 M NaOH at each pH. In accordance to Smedley and Kinniburgh [35], As(III) species prevails at pH between 7 and 10, and a better chemosensor response for As(III) is expected at a neutral pH and/or at slight alkaline pHs. The required amount

of As (III) standard solution (final As(III) concentration between 0 and 50 $\mu\text{g L}^{-1}$) was also prepared in 0.1 M KH_2PO_4 /0.1 M NaOH at the selected pH. Experiments involved the use of 1.5 mL of IIP-QDs solution, and variable volumes of As(III) solutions to obtain As(III) within the 0-50 $\mu\text{g L}^{-1}$ after dilution to 2.0 mL (0.1 M KH_2PO_4 /0.1 M NaOH at the selected pH was used as diluent). RTP intensities were measured after 15 min and results in triplicate are plotted on Figure 4A. Good linearity was observed between 0-20 $\mu\text{g L}^{-1}$, and the highest RTP quenching (highest slope) was observed at pH 7.0, that was chosen for further experiments.

3.2.3. Effect of the IIP-QDs concentration

Several IIP-QDs concentrations (20, 50, 100, 200 and 500 mg L^{-1}) prepared in 0.1M KH_2PO_4 /0.1 M NaOH at pH 7.0 were used to investigate the effect of the IIP-QDs concentration on the As (III) RTP quenching system (As concentrations ranging from 0-20 $\mu\text{g L}^{-1}$). Results are given in Figure 4B, and the highest slope (highest RTP quenching) was obtained when using an IIP-QDs concentration of 20 mg L^{-1} . Additional experiments were further performed with higher As(III) concentrations (50 and 100 $\mu\text{g L}^{-1}$) and higher IIP-QDs concentrations. However, RTP quenching did not increase probably due to nanoparticles aggregation and cloudiness [36]. Therefore, IIP-QDs concentration was fixed at 20 mg L^{-1} .

3.2.4. Interaction between IIP-QDs and As (III) and As (V) species

Although the template used for IIP synthesis (As(III)) was used for optimizing the best conditions for RTP quenching, the effect of both inorganic As species (As(III) and As(V)) were evaluated since a screening RTP probe is expected for total inorganic As (As(III) plus As(V)). The quenching effect of As (III) and As (V) at concentrations within the 0-20 $\mu\text{g L}^{-1}$ range was tested using 20 mg L^{-1} IIP-QDs under optimum conditions (use of 0.1M KH_2PO_4 /0.1M NaOH, pH 7.0 as a diluent and RTP measurement after 15 min). Experiments in triplicate showed slopes of -4.90 ± 0.29 and -4.38 ± 0.65 for As (III) and As (V), respectively. The slightly experimental difference obtained may be due to the quenching effect depending on the recognition cavity generated by the template molecule (NaAsO_2), although the prepared material shows good

recognition properties also for As(V). The quenching effect on IIP-QDs caused by the interaction with As(III) and As(V) within the 0-20 $\mu\text{g L}^{-1}$ range is graphically shown in Figure 5A,B.

3.3. Imprinting effect and selectivity

Several experiments were performed with IIP-QDs and NIP-QDs in the optimum conditions to compare the template (As(III)) responses and responses from other As species [As (V), AsC, AsB, MMA and DMA], and other elements which are present in fish such as microelements (Pb, Cd, Hg) and macro elements (P, K, Na, K, Ca, Mg, Zn, Fe, Co and Cu). The RTP quenching was measured by following Stern–Volmer equation [37].

$$\frac{P_0}{P} = 1 + K_{SV}[C] \quad (1)$$

where P_0 and P are the RTP intensity of the IIP-QDs or NIP-QDs in the absence and presence of the template (As(III)) or other tested elements, $[C]$ is the concentration of As(III) or other tested As species and elements, and K_{SV} is the Stern-Volmer constant.

The effect of the template (As(III)), other As species and microelements was studied up to 20 $\mu\text{g L}^{-1}$; whereas, the quenching effect of macro elements was studied at concentrations up to 100 $\mu\text{g L}^{-1}$. Results are listed in Table 1 and K_{SV} values of 0.0106 for As (III) and 0.0073 for As (V) when using IIP-QDs were calculated. Similar experiments performed by using NIP-QDs have showed negligible interaction between As(III) and As(V) with NIP-QDs (absence of quenching) which prove that RTP quenching occurs only when there are recognition cavities in the IIP layer over the QD nanoparticles.

Recognition properties of the prepared composite through As(V) is attributed to the presence of 1-vinyl imidazole, a bifunctional vinylated compound (acting as monomer and interactive agent) which allows interaction with As(III) and As(V). In the study of Tsoi et al [33], the authors investigated the selectivity and interaction mechanism of As-IIPs polymers based on the polymerization of styrene and the heterocyclic analogues vinylated pyridine and 1-vinyl imidazole (containing one and two nitrogen atoms, respectively). They concluded that 1-vinyl

imidazole based As-IIP has superior selectivity and analyte recognition due to the higher density of arsenic-binding N-functionalities of the monomer. Fontanals et al. [38] also found that vinyl imidazole-DVB resins with a high nitrogen content (higher polarity) retained a bigger amount of polar compounds (phenols, oxamyl, methomyl). Therefore, it seems that the synthesized polymer can retain the template (As(III)) and also might recognize other ions of similar characteristics such as As(V) in the case of the present study. The strength of these interactions with the nitrogen ions would be pH-dependent.

Experiments performed with IIP-QDs and NIP-QDs for other As species (organic As species) as well as for other elements (Table 1) have led to very small K_{SV} constants which implies that the prepared material is quite selective for inorganic As.

Table 1 also lists values regarding imprinting effect (IE as the ratio between K_{SV} for IIP-QDs and K_{SV} for NIP-QDs for each target), and selectivity (SF as the ratio between K_{SV} for IIP-QDs for the template and K_{SV} for IIP-QDs for the element/specie under study), which were calculated in accordance to

$$IE = \frac{K_{SV(IIP)}}{K_{SV(NIP)}} \quad (2)$$

where $K_{SV(IIP)}$ and $K_{SV(NIP)}$ are the Stern–Volmer constants for template and for each element/As specie under study when using IIP-QDs and NIP-QDs, respectively; and the selectivity factor

$$SF = \frac{K_{SV(IIP,As(III))}}{K_{SV(IIP,Q)}} \quad (3)$$

where $K_{SV(IIP,As(III))}$ is the Stern–Volmer constant for template using IIP-QDs, and $K_{SV(IIP,Q)}$ is the Stern–Volmer constant for each element/As specie under study when using IIP-QDs. Similarly, selectivity factors were calculated comparing $K_{SV(IIP,As(III))}$ and the Stern–Volmer constants for each element/As specie under study when using NIP-QDs

$$SF_{NIP} = \frac{K_{SV(IIP,As(III))}}{K_{SV(NIP,Q)}} \quad (4)$$

The calculated IE was 153.4 for As (III) and 91.3 for As(V); whereas IE values were very small (lower than 1.5) for organic As species and other ions (Table 1). These results agree with calculated SF values, which are small for inorganic As, and high for organic As species and other ions. These findings imply that the material's response is quite similar and selective for both inorganic As species, and that the RTP quenching (variable used for quantitative determinations) is only attributed to the presence of As(III) and As(V). In addition, the high IF values for inorganic As species means that RTP quenching is consequence of the presence of specific recognition cavities for As(III) and As(V) in the IIP layer.

3.4. Analytical performances

3.4.1. Calibration and matrix effect

The matrix effect was evaluated by comparing RTP quenching attributed to As(III) in aqueous 0.1M KH₂PO₄/0.1M NaOH, pH 7.0 (external aqueous calibration) and also when mixing fish extracts (standard addition calibration) at several dilution factors (1:10, 1:20 and 1:40, which implies the use of 200, 100 and 50 μ L of a fish extract with IIP-QDs under optimum conditions). The standard addition and external calibration were prepared in three different days and each concentration level was also performed in triplicate. The slopes of the standard addition calibration graphs obtained for several sample dilution ratios were -3.64 ± 0.30 , -2.77 ± 0.11 and -5.59 ± 0.34 for 1:10, 1:20 and 1:40 dilution factors, respectively. The higher slope was observed when using the higher dilution factor (1:40), slope quite similar to that obtained when using external aqueous calibration (-4.90 ± 0.29). There was no significant difference ($p > 0.05$) between external calibration and 1:40 standard addition matrix dilution calibration curve. Hence 1:40 dilution was selected in real sample analysis and this dilution has been found to be adequate for assessing low concentrations of As (III) plus As(V) in fish samples. However, improvements on sensitivity could be obtained by using small dilution factors and the standard addition technique as a calibration method.

3.4.2. Limit of detection and limit of quantification

The limit of detection (LOD) and the limit of quantification (LOQ) were calculated based on EURACHEM [5] guideline as 3σ (σ is a standard deviation of 11 blank readings) for LOD, and as 10σ for LOQ [39]. The RTP intensity of a solution of 1.5 mL of 20 mg L⁻¹ IIP-QDs in 0.1M KH₂PO₄/0.1M NaOH, pH 7.0 plus 0.5 mL of 0.1 M KH₂PO₄/0.1 M NaOH was measured under the previously optimized conditions. Then the standard deviation was divided by the slope of the calibration graph (As(III) as a calibrant), and the calculated LOD and LOQ values were 8.9 and 29.6 µg kg⁻¹, respectively. There was no published guideline for inorganic As levels present in fish species; however, there is a published guidance for inorganic As in rice products [40]: 0.20 mg kg⁻¹ for non-parboiled milled rice, 0.25 mg kg⁻¹ for parboiled rice and husked rice, 0.30 mg kg⁻¹ for rice waffles, rice wafers, rice crackers and rice cakes, and 0.10 mg kg⁻¹ for rice destined for the production of food for infants and young children. The calculated LOD and LOQ values are lower than the established maximum values by the EU/EC regulations.

3.4.3. Precision and accuracy

Inter-day and intraday precision was assessed by using an aqueous calibration method (1:40 dilution which implies absence of matrix effect). Three As(III) concentration levels (1.0, 5.0 and 20 µg L⁻¹) were measured seven times in three different days for inter-day assays, and all concentration levels (1.0, 2.0, 5.0, 10 and 20 µg L⁻¹) were measured in triplicate on seven consecutive days for intraday assays. Results (Table 2) show relative standard deviations (RSD) lower than 11% for inter-day precision, and lower than 7% for intraday assays. RSD for all the levels was below 10%. According to published method validation guidance [41], good precision is attained when RSD values are lower than 20%, which means that the proposed method shows good inter-day and intraday precision.

Regarding analytical recovery, inter-day assays show values within the 105-107% range; whereas, intraday analytical recovery varied from 98 to 103%. All values are close to 100% which also implies good analytical recovery for inter-day and intraday assays.

A CRM (BCR-668) showing certified total As concentration was analysed for total As assessment (microwave assisted acid digestion and ICP-MS measurement). Results are given in Table 3, and good accuracy has been observed for total As determination (found total As concentration within the certified total As concentration range). However, the BCR-668 has not been certified for total inorganic As neither for single As(III) and As(V) species. Therefore, this CRM was subjected to the proposed RTP method for assessing total inorganic As (As(III) plus As(V)) and also to HPLC-ICP-MS (single As(III) and As(V) concentrations), and results (total inorganic As) have been found quite similar when applying both determination techniques (Table 3).

3.5. Applications

The developed method was applied to five fish samples to assess total inorganic As (As(III) plus As(V)). In addition, the same fish samples were analysed by HPLC-ICP-MS for assessing single As(III) and As(V) concentrations, and total As concentration was also determined by ICP-MS after a microwave assisted acid digestion procedure. Each sample was analysed in triplicate, and results are tabulated in Table 3. A paired sample t-test (95% confidence interval) was applied to compare total inorganic As by the proposed RTP method and by HPLC-ICP-MS (sum of single As(III) and As(V) concentrations). There was no significant differences between the results obtained using both methods since the calculated t ($t_{\text{cal}}=0.647$) was lower than the tabulated t ($t_{\text{tab}}=2.78$) at a 95% confidence level ($P>0.05$), four degrees of freedom.

Conclusions

The developed RTP method based on IIP-QDs has been found to be highly sensitive, allowing the selective assessment of toxic arsenic (inorganic arsenic) in fish by using low-cost laboratory instrumentation. The use of vinyl imidazole as a complexing agent has been useful so that the IIP can recognize both As (III) and As (V) ions, allowing a simultaneously determination of both

toxic arsenic species. Other arsenic species (organoarsenic compounds) as well other ions do not interact with the prepared composite material, and RTP quenching is only attributed to the inorganic As species (As(III) plus As(V)). Under the optimum conditions, the composite RTP-based **chemosensor** allowed the accurate determination of total inorganic arsenic in several fish samples and in the BCR-668 CRM (values statistically comparable with those obtained after applying a high expensive instrumentation such as HPLC-ICP-MS). The current method has therefore several advantages such as being a simple procedure with high selectivity and stability, low cost, short analysis time and sensitive (low LOD/LOQ), and may offer a new approach to the development of low-cost and sensitive methods for trace As level monitoring in other foodstuff and biological materials.

Acknowledgment

This work was supported by the *Dirección Xeral de I+D – Xunta de Galicia Grupos de Referencia Competitiva* (project number 6RC2014/2016 and ED431C2018/19), and Development of a Strategic Grouping in Materials - AEMAT (grant ED431E2018/08). Authors thanks to Dr. Bruno Dacuña-Mariño (*Unidade de Raios X*) at *Rede de Infraestruturas de Apoio á Investigación e ao Desenvolvemento Tecnolóxico* – University of Santiago de Compostela) for XRD technical support, to Eugenio Solla (*Servicio de Microscopía Electrónica*) at CACTI– University of Vigo for TEM/EDS technical support, and to Dr. María Celeiro (LIDSA, Department of Analytical Chemistry, Nutrition and Bromatology – University of Santiago de Compostela) for ASE technical assistance.

Disclosure statement

The authors declare no conflicts of interest

Table 1: Stern-Volmer constants, imprinting effect and selectivity factors (IIP-QDs and NIP-QDs) for As(III), As(V), organic As species, and other ions

	$K_{SV(IIP)}$ a	$K_{SV(NIP)}$ a	Imprinting effect ($K_{SV(IIP)}/K_{SV(NIP)}$)	Selectivity factor, SF, ($K_{SV(IIP)}$, $As(III)/K_{SV(IIP,Q)}$)	Selectivity factor SF _{NIP} ($K_{SV(IIP)}$, $As(III)/K_{SV(NIP,Q)}$)
As(III)	0.0106	0.00007	151.4	–	21.2
As(V)	0.0073	0.00008	91.3	1.45	132
AsB	0.00005	0.002	0.025	212.	5.3
AsC	0.0004	0.0018	0.22	26.5	5.9
MMA	0.0008	0.0012	0.67	13.3	8.8
DMA	0.0016	0.0018	0.89	6.6	5.9
Hg	0.0008	0.0026	0.31	13.2	4.1
Pb	0.0009	0.0009	1.00	11.8	11.8
Cd	0.001	0.001	1.00	10.6	10.6
P	0.0003	0.0002	1.50	35.3	53.0
K	0.00005	0.0003	0.17	212	35.3
Ca	0.0001	0.0006	0.17	106	17.7
Mg	0.0005	0.0004	1.25	21.2	26.5
Na	0.0022	0.0009	2.44	4.8	11.8
Zn	0.0011	0.0019	0.58	9.6	5.6
Fe	0.0007	0.0004	1.75	15.1	26.5
Co	0.0002	0.0003	0.67	53.0	35.3
Cu	0.0006	0.001	0.60	17.7	10.6

(a) $K_{SV(IIP)}$ and $K_{SV(NIP)}$: Stern–Volmer constants for the template and for each element/As specie under study when using IIP-QDs and NIP-QDs, respectively

Table 2: Intra-day and inter-day precision (RSD %) and analytical recovery (AR %) of the method

Parameter	Concentration ($\mu\text{g L}^{-1}$)	As(III)	
		AR (%)	RSD (%)
Inter-day (n=7)	1	107±1	5
	5	105±1	11
	20	107±2	10
Intraday (n=7)	1	101±10	4
	2	103±11	5
	5	102±5	6
	10	98±7	7
	20	101±3	5

Table 3: Total As and total inorganic As (mean \pm SD, n=3) in BCR-668 and fish samples

Sample	Total As (mg kg ⁻¹) ^a	Inorganic As (mg kg ⁻¹) ^b	Inorganic As (mg kg ⁻¹) ^c
BCR-668 (certified value)	7.1 \pm 0.5	–	–
BCR-668 (found value)	6.8 \pm 0.1	0.54 \pm 0.05	0.58 \pm 0.02
Swordfish-1	0.60 \pm 0.02	0.37 \pm 0.06	0.37 \pm 0.01
Swordfish-2	1.79 \pm 0.09	0.34 \pm 0.03	0.35 \pm 0.04
Yellowfin tuna	1.98 \pm 0.02	0.29 \pm 0.02	0.28 \pm 0.02
Blue shark	4.94 \pm 0.30	0.99 \pm 0.09	0.95 \pm 0.02
Cod	0.34 \pm 0.02	0.02 \pm 0.01	0.03 \pm 0.01

^a Microwave assisted acid digestion followed by ICP-MS determination

^b Inorganic As: Sum of As(III) and As(V) measured by HPLC-ICP-MS

^c Inorganic As: As(III) plus As(V) measured by IIP-QDs based RTP

Figures' captions

Figure 1: Schematic procedure for the synthesis of Mn-ZnS@SiO₂ QDs and IIP-Mn-ZnS@SiO₂ QDs

Figure 2: Fourier transform infra-red spectra for IIP-QDs (with and without template), and NIP-QDs

Figure 3: TEM analysis for NIP-QDs (A), IIP-QDs before template removal (B), and IIP-QDs after template removal (C)

Figure 4: Effect of the pH (A) and IIP-QDs concentration (B) on the RTP quenching by As (III) concentration

Figure 5: RTP quenching of IIP-QDs concentration in presence of increasing concentrations of As(III) (A) and As(V) (B)

Figure 1

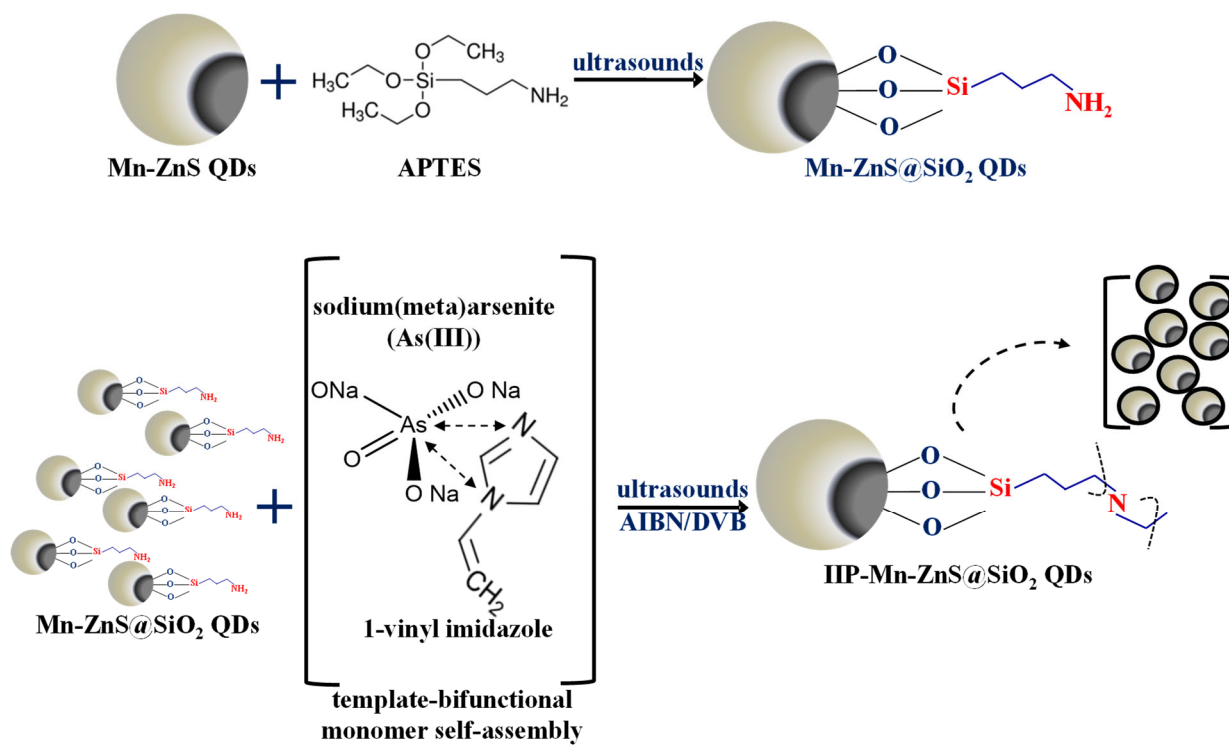


Figure 2

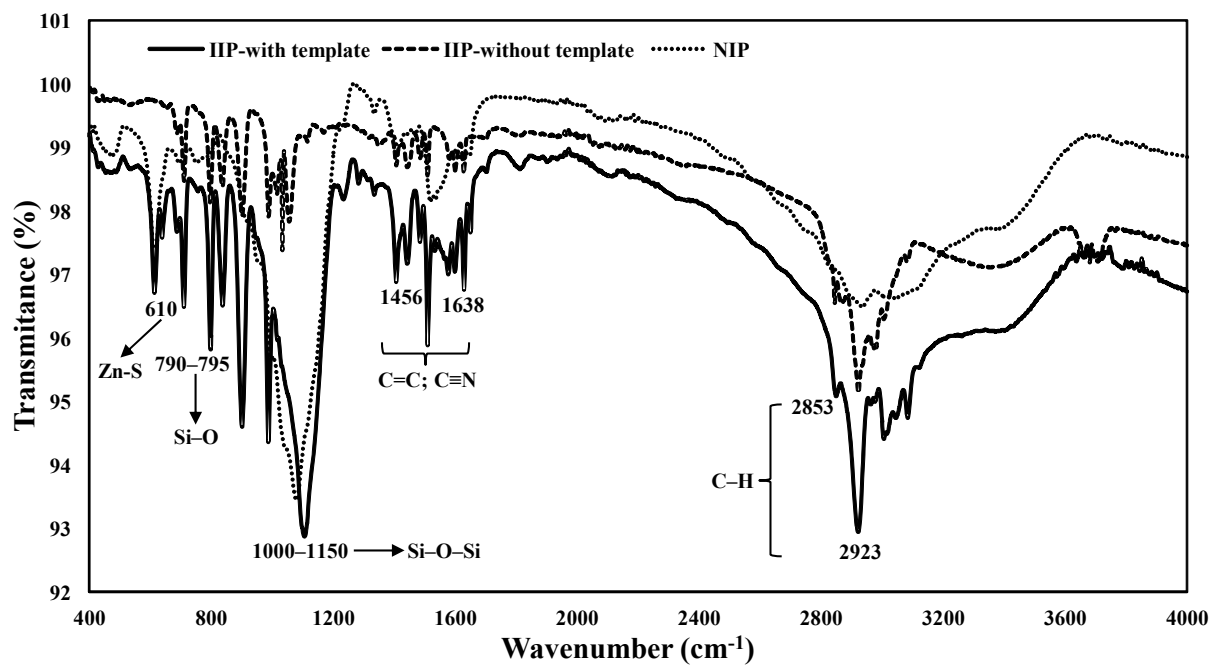


Figure 3

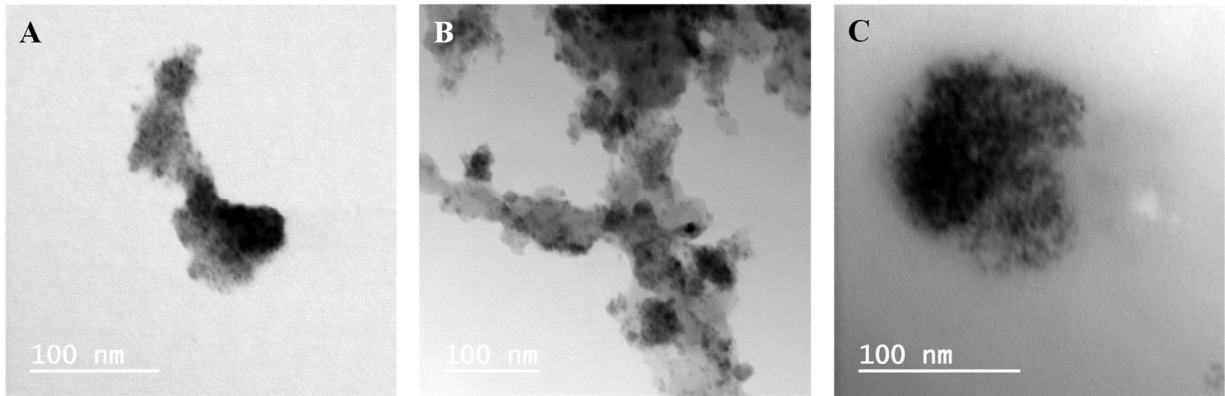


Figure 4

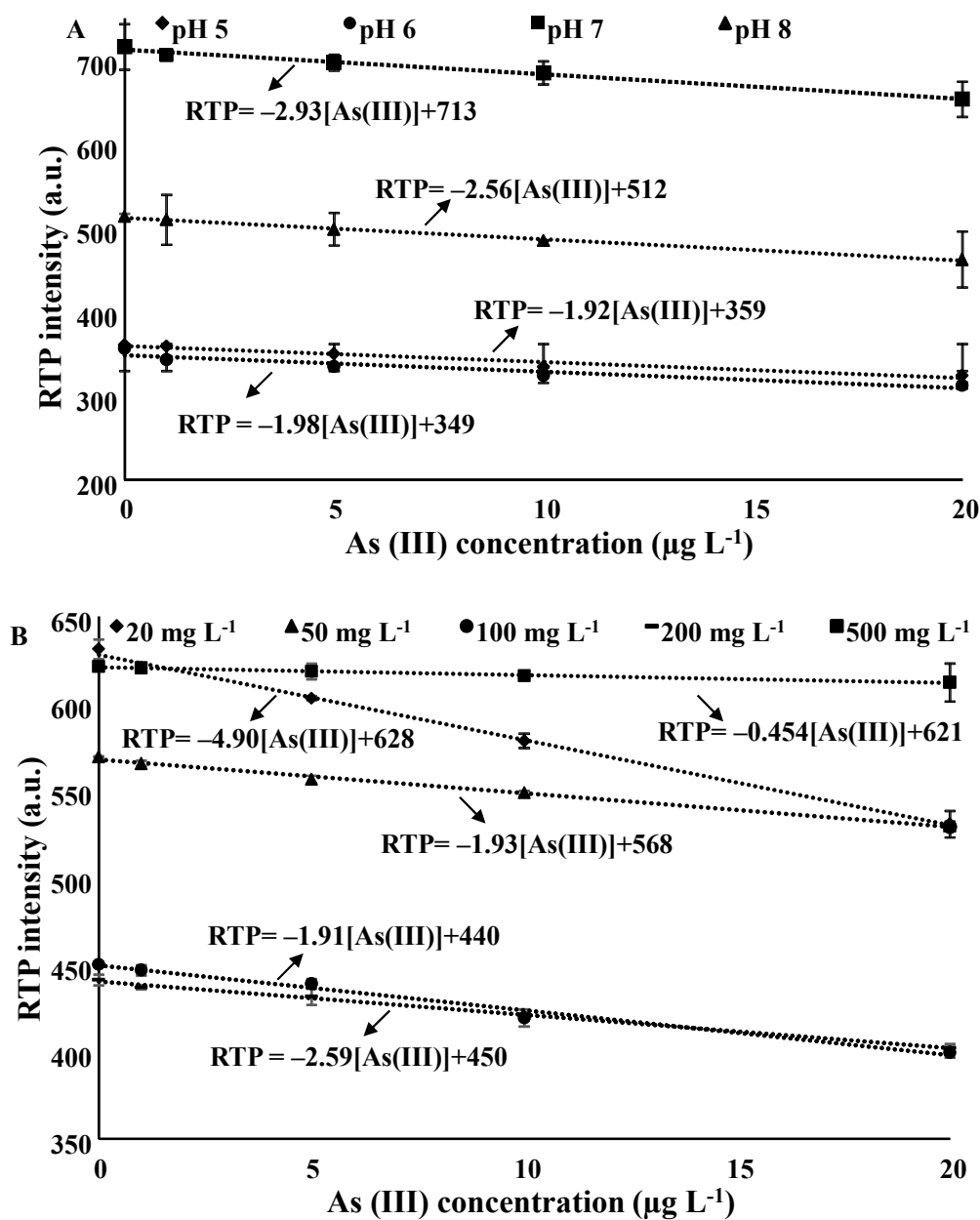
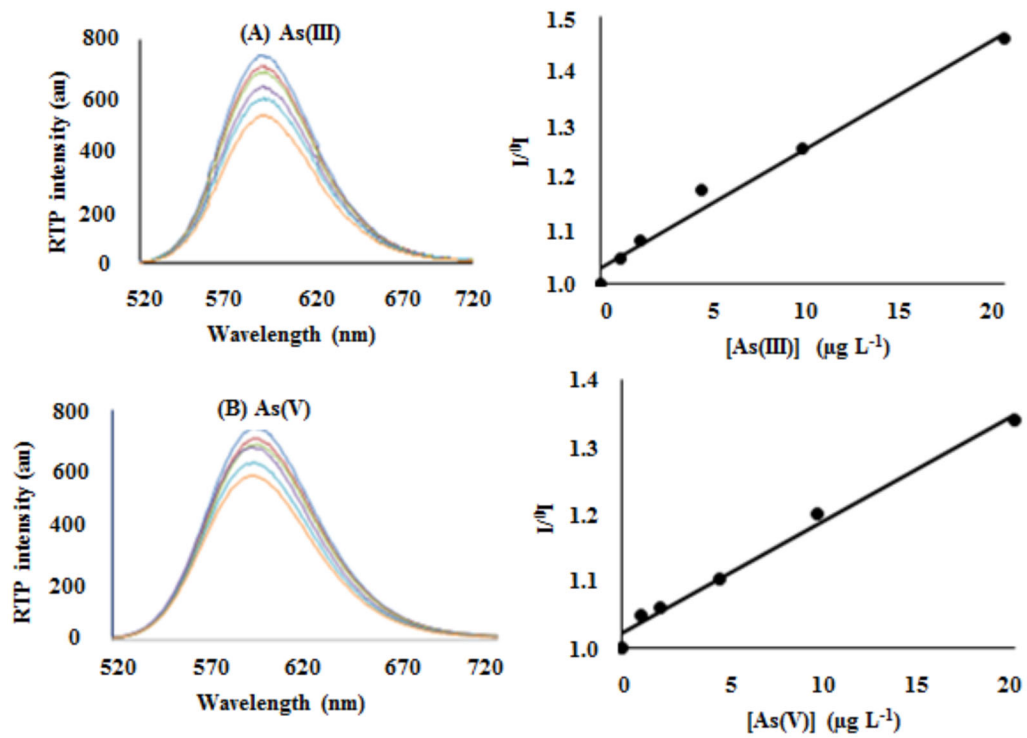


Figure 5



Electronic Supplementary Information (ESI)

Electronic Supplementary Information (ESI)

Synthesis and application of a surface ionic imprinting polymer on silica-coated Mn-doped ZnS quantum dots as a chemosensor for the selective detection of inorganic arsenic in fish

Kamal K Jinadasa, Elena Peña-Vázquez, Pilar Bermejo-Barrera, Antonio Moreda-Piñeiro

Table S1. HPLC-ICP-MS operating conditions

ICP-MS	
Radio frequency power (W)	1600
Ar flow rate (plasma/auxiliary/nebulizer) (L/min)	16/1.2/0.92
KED mode, He flow rate (mL/min)	4
Integration time (ms)	250
Dwell time (ms)	443000
Mass monitored	⁷⁵ As
HPLC	
Column	Hamilton PRP×100, 10 μm, 4.1×100 mm
Mobile phase	(NH ₄)H ₂ PO ₄ , 15 mmol, pH 6.0
Flow rate	1 mL min ⁻¹ , 8.5 min
Injection volume	20 μL

Table S2. Operating ICP-MS conditions for total As determination in acid digests from fish samples.

Operating ICP-MS conditions		
Radiofrequency power		1600 W
Gas flows	Nebulization	0.92 mL min ⁻¹
	Auxiliary	1.2 mL min ⁻¹
	Plasma	16 mL min ⁻¹
KED mode: He flow rate/		
mL min ⁻¹	4.0	
Analyte	⁷⁵ As	
Internal standard	⁷⁴ Ge	

Figure S1: XRD spectra for IIP-QDs (with and without template), and NIP-QDs

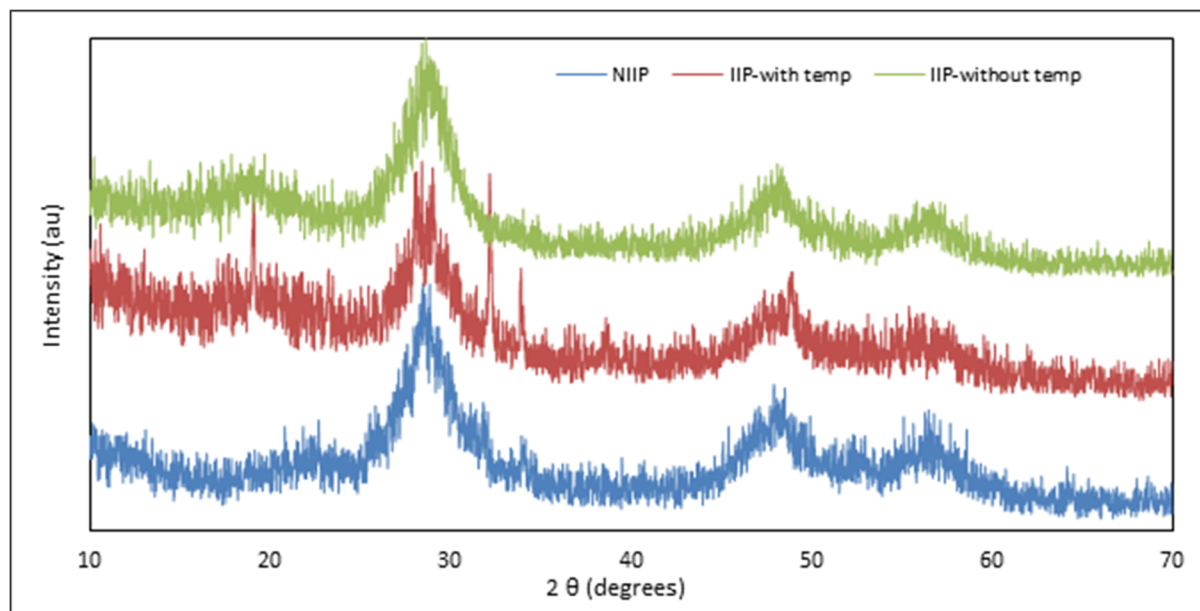
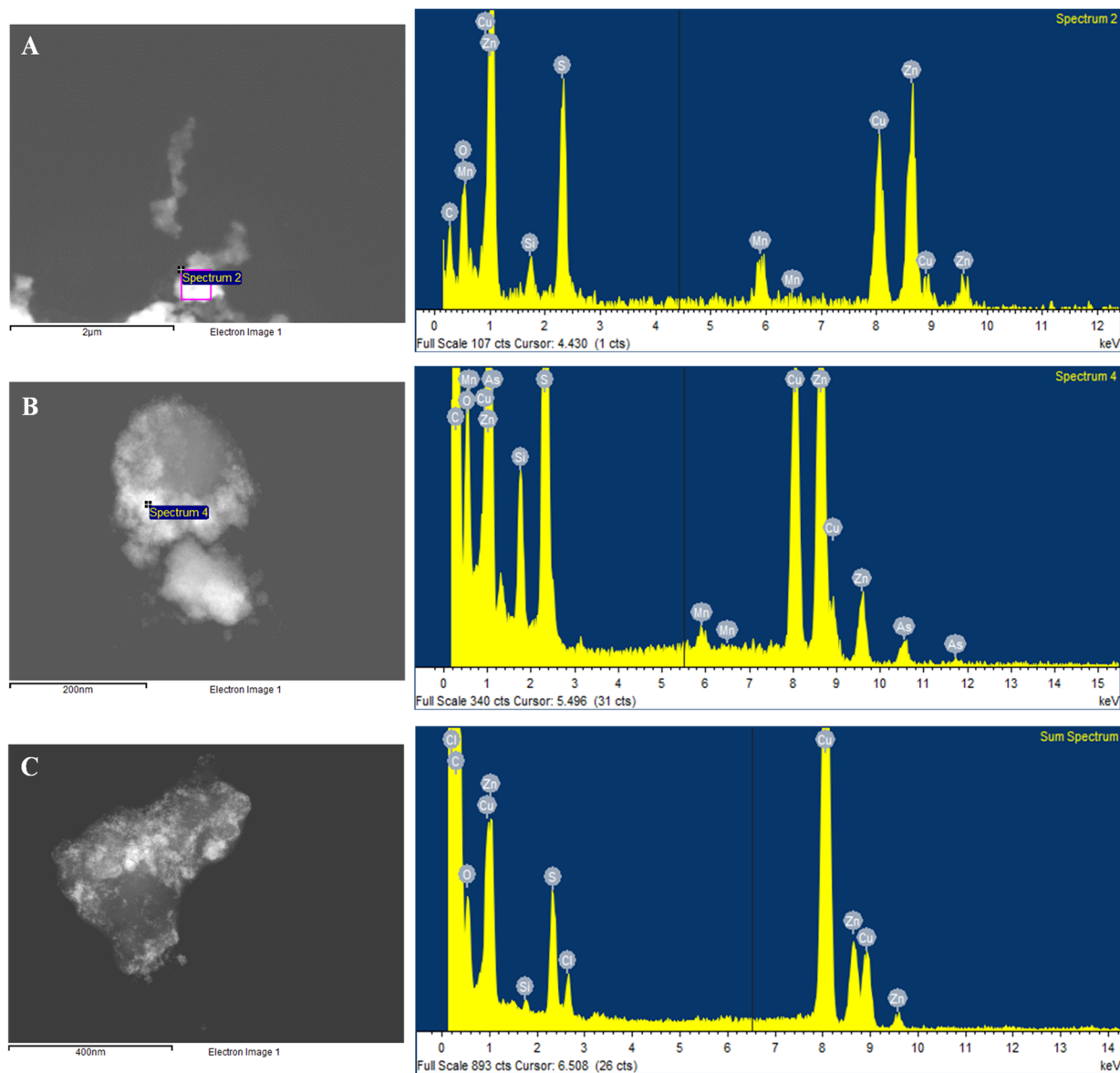


Figure S2: TEM-EDS analysis for NIP-QDs (A), IIP-QDs before template removal (B), and IIP-QDs after template removal (C)



References

- [1] Liu CW, Liang, CP, Huang, FM, Hsueh, YM. Assessing the human health risks from exposure of inorganic arsenic through oyster (*Crassostrea gigas*) consumption in Taiwan. *Sci. Total Environ.* 2006;361: 57-66.
- [2] ATSDR (2017) ATSDR's Substance Priority List. Agency for Toxic Substances and Disease Registry. <https://www.atsdr.cdc.gov/SPL/>. Accessed 20 December 2018.
- [3] IARC (2018) IARC monographs on the evaluation of carcinogenic risk to human. <https://monographs.iarc.fr/list-of-classifications-volumes/>. Accessed 29 December 2018.
- [4] Tidwell JH, Allan GH. Fish as a food: Aquaculture's contribution. *EMBO reports* 2001; 2(11): 958-963
- [5] Meharg AA, Lombi E, Williams PN, Scheckel KG, Feldmann J, Raab A, Zhu Y, Islam R. Speciation and localization of arsenic in white and brown rice grains. *Environ. Sci. Tech.* 2008;42:1051-1057.
- [6] Gao Y, Baisch P, Mirlean N, Rodrigues da Silva JFM, Van Larebeke N, Baeyens W, Leermakers M. Arsenic speciation in fish and shellfish from the North Sea (Southern bight) and Açu Port area (Brazil) and health risks related to seafood consumption. *Chemosphere* 2018;191:89-96.
- [7] Wei X, Zhou Z, Dai J, Hao T, Li H, Xu Y, Gao L, Pan J, Li C, Yan Y. Composites of surface imprinting polymer capped Mn-doped ZnS quantum dots for room-temperature phosphorescence probing of 2,4,5-trichlorophenol. *J. Lumin.* 2014;155: 298-304.
- [8] Wang YQ, Zou WS. 3-Aminopropyltriethoxysilane-functionalized manganese doped ZnS quantum dots for room-temperature phosphorescence sensing ultratrace 2,4,6-trinitrotoluene in aqueous solution. *Talanta* 2011;85:469-475.
- [9] Peng X, Manna L, Yang W, Wickham J, Scher E, Kadavanich A, Alivisatos AP. Shape control of CdSe nanocrystals. *Nature* 2000;404: 59-61.

-
- [10] Valizadeh A, Mikaeili H, Samiei M, Farkhani SM, Zarghami N, Kouhi M, Akbarzadeh A, Davaran S. Quantum dots: synthesis, bioapplications, and toxicity. *Nanoscale Res. Lett.* 2012; <http://www.nanoscalereslett.com/content/7/1/480>.
- [11] Costas-Mora I, Romero V, Lavilla I, Bendicho C. An overview of recent advances in the application of quantum dots as luminescent probes to inorganic-trace analysis. *Trends Anal. Chem.* 2014;57:64-72.
- [12] Sotelo-Gonzalez E, Fernandez-Argüelles MT, Costa-Fernandez JM, Sanz-Medel A. Mn-doped ZnS quantum dots for the determination of acetone by phosphorescence attenuation. *Anal. Chim. Acta* 2012;712:120-126.
- [13] Zhang C, Zhang K, Zhao T, Liu B, Wang Z, Zhang Z. Selective phosphorescence sensing of pesticide based on the inhibition of silver(I) quenched ZnS:Mn²⁺ quantum dots. *Sensor Actuat. B-Chem.* 2017;252:1083-1088.
- [14] Gan T, Zhao N, Yin G, Liu J, Liu W. Mercaptopropionic acid-capped Mn-doped ZnS quantum dots and Pb²⁺ as sensing system for rapid and sensitive room-temperature phosphorescence detection of sulfide in water. *J. Photoch. Photobio. A* 2018;364:88-96.
- [15] Tan L, Li Y, Tang Y, Kang C, Yu Z, Xu S. Room temperature phosphorescence sensor for Hg²⁺ based on Mn-doped ZnS quantum dots. *J. Nanosci. Nanotechnol.* 2012;12:7788-7795.
- [16] Chen J, Zhu Y, Zhang Y. Glutathione-capped Mn-doped ZnS quantum dots as a room-temperature phosphorescence sensor for the detection of Pb²⁺ ions. *Spectrochim. Acta A* 2016;164:98-102.
- [17] Deng P, Lu LQ, Cao WC, Tian XK. Phosphorescence detection of manganese(VII) based on Mn-doped ZnS quantum dots. *Spectrochim. Acta A* 2017;173:578-583.
- [18] Chen L, Wang X, Lu W, Wu X, Li J. Molecular imprinting: Perspectives and applications. *Chem. Soc. Rev.* 2016;45:2137-2211
- [19] Fu J, Chen L, Li J, Zhang Z. Current status and challenges of ion imprinting, *J. Mater. Chem. A* 2015;3:13598-13627.

-
- [20] Niu M, Pham-Huy C, He H. Core-shell nanoparticles coated with molecularly imprinted polymers: a review. *Microchim. Acta* 2016;183:2677–2695.
- [21] Liu G, Huang X, Li L, Xu X, Zhang Y, Lv J, Xu D. Recent advances and perspectives of molecularly imprinted polymer-based fluorescent sensors in food and environment analysis. *Nanomaterials* 2019;9;1030; doi:10.3390/nano9071030.
- [22] Qi J, Li B, Wang X, Zhang Z, Wang Z, Han J, Chen L. Three-dimensional paper-based microfluidic chip device for multiplexed fluorescence detection of Cu²⁺ and Hg²⁺ ions based on ion imprinting technology. *Sensor. Actuat. B-Chem.* 2017;251:224-233.
- [23] Zhang MY, Huang RF, Ma XG, Guo LH, Wang Y, Fan YM. Selective fluorescence sensor based on ion-imprinted polymer-modified quantum dots for trace detection of Cr(VI) in aqueous solution. *Anal. Bioanal. Chem.* 2019;411:7165-7175.
- [24] Chantada-Vázquez MP, Sánchez-González J, Peña-Vázquez E, Tabernero MJ, Bermejo AM, Bermejo-Barrera P, .Moreda-Piñeiro A. Synthesis and characterization of novel molecularly imprinted polymer – coated Mn-doped ZnS quantum dots for specific fluorescent recognition of cocaine. *Biosen. Bioelectron.* 2016,75:213-221.
- [25] Ren X, Chen L. Quantum dots coated with molecularly imprinted polymer as fluorescence probe for detection of cyphenothrin. *Biosen. Bioelectron.* 2015,64:182-188.
- [26] Piao Y, Burns A, Kim J, Wiesner U, Hyeon T. Designed fabrication of silica-based nanostructured particle systems for nanomedicine applications. *Adv. Funct. Mater.* 2008;18:3745-3758.
- [27] Zhi K, Wang L, Zhang Y, Jiang Y, Zhang L, Yasin A. Influence of size and shape of silica supports on the sol–gel surface molecularly imprinted polymers for selective adsorption of gossypol. *Materials* 2018, <https://doi.org/10.3390/ma11050777>.
- [28] Yi DK, Selvan ST, Lee SS, Papaefthymiou GC, Kundaliya D, Ying JY. Silica-coated nanocomposites of magnetic nanoparticles and quantum dots. *J. Am. Chem. Soc.* 2005;127:4990-4991.

-
- [29] Darbandi M, Thomann R, Nann T. Single quantum dots in silica spheres by microemulsion synthesis. *Chem. Mater.* 2005;17:5720-5725.
- [30] Wei X, Zhou Z, Hao T, Li H, Xu Y, Lu K, Wu Y, Dai J, Pan J, Yan Y. Highly-controllable imprinted polymer nanoshell at the surface of silica nanoparticles based room-temperature phosphorescence probe for detection of 2,4-dichlorophenol. *Anal. Chim. Acta* 2015;870:83-91
- [31] Babamiri B, Salimi A, Hallaj R. Switchable electrochemiluminescence aptasensor coupled with resonance energy transfer for selective attomolar detection of Hg^{2+} via CdTe@CdS/dendrimer probe and Au nanoparticle quencher. *Biosen. Bioelectron.* 2018;102:328-335.
- [32] Tsoi YK, Ho YM, Leung KSY. Selective recognition of arsenic by tailoring ion-imprinted polymer for ICP-MS quantification. *Talanta* 2012;89:162-168.
- [33] Mohaghehpour E, Moztarzadeh F, Rabiee M, Tahriri M, Ashuri M, Sameie H, Salimi R, Moghadas S. Micro-emulsion synthesis, surface modification, and photophysical properties of nanocrystals for biomolecular recognition. *IEEE Nanobiosci.* 2012;11:317-323.
- [34] Uzuriaga-Sánchez RJ, Wong A, Khan S, Pividori MI, Picasso G, Sotomayor MDPT, Synthesis of a new magnetic-MIP for the selective detection of 1-chloro-2,4-dinitrobenzene, a highly allergenic compound. *Mater. Sci. Eng. C* 2017;74:365-373.
- [35] Smedley PL, Kinniburgh DG, A review of the source, behaviour and distribution of arsenic in natural waters. *Appl. Geochem.* 2002;17:517-568.
- [36] Verma N, Singh AK, Saini N. Synthesis and characterization of ZnS quantum dots and application for development of arginine biosensor. *Sens. Biosensing Res.* 2017;15:41-45.
- [37] Li H, Li Y, Cheng J. Molecularly imprinted silica nanospheres embedded CdSe quantum dots for highly selective and sensitive optosensing of pyrethroids. *Chem. Mater.* 2010;22:2451-2457.
- [38] Fontanals N, Marcé RM, Galià M, Borrull F. Synthesis of hydrophilic sorbents from *N*-vinylimidazole/divinylbenzene and the evaluation of their sorption properties in the solid-phase extraction of polar compounds. *J. Polym. Sci. Pol. Chem.* 2004;42: 2019–2025.

[39] EURACHEM (2014) The Fitness for purpose of Analytical methods. 2 ed.: EURACHEM

[40] EU/EC 1006/2015. Commission Regulation (EC), No 2015/1006 of amending Regulation (EC) No 1881/2006 as regards maximum levels of inorganic arsenic in foodstuffs Official journal of European Union, L161, 14-16.

[41] SANTE 2017. (11813) Guidance document on analytical quality control and method validation procedures for pesticide residues and analysis in food and feed: European Commission.